

Development and whirltortest of the SMART active flap rotor

Friedrich K. Straub, Dennis K. Kennedy, Alan D. Steimle, V. R. Anand, and Terry S. Birchette
The Boeing Company, Mesa, Az 85215

ABSTRACT

A full scale Smart Material Actuated Rotor Technology (SMART) system with piezoelectric actuated blade flaps was developed and whirltortested. The development effort included design, fabrication, and component testing of rotor blades, trailing edge flaps, piezoelectric actuators, switching power amplifiers, and the data/powersystem. Simulations and model scale wind tunnel tests have shown that this system can provide 80% vibration reduction, 10 dB noise reduction for a helicopter passing overhead, and substantial aerodynamic performance gains. Whirltortesting of the 34-foot diameter rotor demonstrated the functionality, robustness, and required authority of the active flap system.

The program involved extensive development work and risk reduction tests which resulted in a robust, high performance actuator and tightly integrated actuator, flap, and blade system. The actuator demonstrated excellent performance during bench testing and has accumulated over 60 million cycles under a spectrum of loading conditions. The flight worthy active flap rotor blades were based on a modified design of the FAACertified MD900 Explorer production rotor blade. Whirltortesting was conducted with full rotor instrumentation and a 5-1/2 hour operation. The rotor was tested for 13 hours of flap operation. Flap inputs included open loop static and dynamic commands. The flaps showed excellent authority with oscillatory thrust greater than 10% of the steady baseline thrust. Various flap actuation frequency sweeps were run to investigate the dynamics of the rotor and the flap system. Limited closed loop tests used hub accelerations and hub loads for feedback.

Proving the integration, robust operation, and authority of the flap system were the key objectives met by the whirltortest. This success depended on tailoring the piezoelectric materials and actuator to the application and meeting actuator/blade integration requirements. Test results demonstrate the feasibility and practicality of applying smart materials for limited authority, active control on a helicopter rotor. Follow-on forward flight demonstrations are needed to quantify the expected significant improvements in vibrations, noise, and aerodynamic performance. Extension of this technology are a prime candidate for on-blade flight control, i.e. elimination of the washplate.

This program was performed as part of DARPA's Smart Materials and Structures Demonstrations. Funding was provided by DARPA, The Boeing Company, NASA, and the U.S. Army. Additional cost share funds were provided by the University of Maryland, MIT, and UCLA.

Keywords: Smart materials, piezoelectric, actuator, helicopter, blade, flap, vibration control, noise control

1. INTRODUCTION

Vibration, noise, and aerodynamic design compromise continue as barriers to further improvements in effectiveness and public acceptance of the helicopter. Blade trailing edge flaps actuated by in-blade smart material actuators have emerged as a primary candidate to dynamically alter the blade structure and apply limited authority active control to achieve significant improvements in rotorcraft performance and mission capability [1-5]. Simulations and model scale wind tunnel tests have shown that this system can provide more than 80% vibration reduction, 10 dB noise reduction for a helicopter passing overhead, and substantial aerodynamic performance gains. Resulting benefits include jetsmooth ride, improved community acceptance, as well as significantly improved lifecycle cost, productivity, and fleet readiness.

Presented at SPIE's Intl. Symposium on Smart Structures and Materials, San Diego, CA, March 14-18, 2004.

The overall program objective was to develop the technology and demonstrate that smart material actuated flaps are feasible and practical for high bandwidth, limited authority active control of a helicopter main rotor. The MD900 Explorer twin engine, light utility helicopter was selected as demonstration vehicle. Its state-of-the-art 5-bladed composite, bearingless main rotor system was modified to include in-blade piezoelectric actuators and trailing edge flaps, Figure 1.

Concept development and design support tests were conducted during Phase I of this program [6]. The current Phase II effort included design, fabrication, and component testing of flight worthy hardware and whirl tower testing of the integrated system. Primary components of the system include the blades, flaps, piezoelectrics, actuators, switching power amplifiers, and data/power system. Their development and results of the whirl tower test are presented here. Additional details of the work performed under Phase II can be found in Reference 7-17.

2. ROTOR BLADE AND FLAP DEVELOPMENT

The basic characteristics of the SMART rotor are shown in Table 1. Primary design objectives for the blade and the flap were to minimize actuation requirements, match the baseline blade dynamics, and minimize weight. A key constraint was to use the production blade tooling with only minor modifications. Secondary design objectives were simplicity, modularity, and the flexibility of the blade to serve as a test bed for alternate actuators.

The blade design was modified to carry the actuator flap. A short link connects the actuator and flap. Details of the blade, flap, and actuator integration are shown in Figures 2-4. The overall layout of the hardware components is shown in Figure 5. Several changes were made to the blade construction, including replacement of the outer veils, and use of flight weight honeycomb core in the mid-section of the blade. Reinforcement was added to provide attachments for the actuator cavity access cover, Figure 6, the actuator mounts, and supports, Figure 7. Leading edge weight was added to maintain chordwise balance, Figure 8. Blade internal wiring was provided for actuator data and power.

The flap parameters, Table 2, were chosen to minimize actuation requirements. Because of the flap length, three intermediate flap supports are required to carry the flap loads. The flap is aerodynamically balanced in order to lower the aerodynamic hinge moment and thus the actuator force required. The flap is also mass balanced. For maximum torsional stiffness the flap is constructed using ± 45 deg graphite plys. The radial allocation was chosen to provide both vibration and noise reduction. Centrifugal loads are transmitted to the blade using gate tension-torsion rod. A series of tests were conducted on the flap, flap link, and tension-torsion rod to confirm properties and to provide qualification data.

A prototype blade, flap, and actuator were fabricated and used to confirm fit and function. Integrated assembly together with a switching amplifier prototype established the validity of the design. Actuator performance under a range of blade deformations showed no degradation. Blade stiffness and free-free tests confirmed that the complete blade assembly, including flap and actuator, closely matched the baseline blade.

3. PIEZOELECTRIC ACTUATOR AND AMPLIFIER DEVELOPMENT

Actuator design considerations include a high energy density, high bandwidth smart material to meet actuation requirements, an efficient mechanism to provide torque amplification and minimize losses, and low volume. In particular the actuator height must be small to fit inside the blade spar. Furthermore, the actuator must be robust and withstand the blade elastic deformations and dynamic loading of 650g steady and ± 30 g cyclic. Model scale rotor tests were conducted and established the feasibility of using piezoelectric actuated blades. A series of tests were conducted and established the feasibility of using piezoelectric actuated blades. Aerelastic simulations showed that ± 2 deg flap deflection is sufficient for vibration reduction at high speed and for noise reduction [6, 9, 10]. This corresponds to an actuator output of ± 43 lb and ± 0.032 in, including some allowance for losses. For design purposes an nominal flap deflection of ± 4 deg with an actuator output of ± 63 lb and ± 0.062 in

were used. Maximum operating frequency was chosen as the rotor (N+1)/rev, i.e. 6/rev or 40 Hz for this 5-bladed rotor, as required for vibration reduction.

Piezoelectric stack actuators were selected as the driving element. Several low and high voltage stacks were tested to determine flexibility with respect to fabrication of different geometries. A custom made, high voltage stack was selected. A number of these stacks were extensively tested under a range of electrical, mechanical, and thermal conditions. Both performance and fatigue tests were run at elevated field levels (2.9 kV/mm) and mechanical preloads were applied. These tests demonstrated that domain wall movement within the piezoelectric ceramics can be used without any significant degradation over 150 million cycles of operation.

The actuator mechanism was based on the x-frame concept [7] with two actuators working in parallel, the frame actuator. The two x-frames are actuated in a push-pull mode. The actuator provides stroke amplification, a means for preloading the piezo-ceramic stacks, and provisions for mounting in the blade. Three prototypes were fabricated and tested to optimize performance and durability. The first prototype used low voltage stacks and validated the concept [17]. It had marginal performance but showed excellent obustness during spin testing. The second prototype was scaled up by 15% and used custom high voltage stacks, Figure 9. Several features were added to facilitate assembly, enhance wear characteristics, and improve mounting in the blade. A third prototype with improved structural characteristics was developed, Figure 10. It demonstrated excellent performance during bench testing, Table 3, and accumulated 66 million cycles under representative electrical and mechanical load conditions. This corresponds to 560 hours of operation at 5/rev. The actuator and bench test rig are shown in Figure 11.

As switching power amplifier was developed to drive the piezoelectric actuator. IGBT (Insulated-Gate Bipolar Transistor) switching at 20 kHz and capacitive energy storage [18] provided the efficiency required to meet the volume and weight constraints for flight testing. In terms of power density it represents a four-fold increase compared to previous models. The amplifier maximum output was -300/+1200 V and 3 A for capacitive loads of 4 μF. A prototype amplifier was developed and used to drive the flaps system. Based on test results, the design was enhanced by adding noise suppression filters, providing better thermal protection for flight testing on hot days, and improving modularity.

4. FLIGHT HARDWARE FABRICATION AND TESTING

A complete set of 5 flight worthy blades, flaps, actuators, and amplifiers was fabricated for whirl testing. In addition to a spare actuator and a spare blade for future pressurized testing, five actuators and amplifiers were tested on the bench to establish performance, stiffness, and natural frequencies. In addition they were run for one hour to seat the components, let the preloads settle, and break in the flap link rod end bearing. After installation in the blade, the actuator/flaps system was run to establish baseline performance, natural frequencies, and to break in the flap bearing surfaces. The blade installed actuator/flaps system had a natural frequency of 98 Hz. The pitch inertias of all flaps and the free-free frequencies and pitch inertias of the mass balanced blade assemblies were also determined. The overall blade weight increased by 5 lb, an increase of 9% in weight and 15% in spanwise moment compared to the baseline blade. The chordwise CG remained unchanged at 27.4%. The completed blade assembly is shown in Figure 12.

5. WHIRL TOWER TEST

Whirl tests were conducted at Mesa in a whirl cage using the Large Rotor Test Stand (LRTS). The LRTS includes a 1500 HP motor, transmission, strut assembly, a 5-component rotor balance, and the rotor flight controls, Figure 13. This test stand has been used in a number of whirl tower and wind tunnel tests of several different rotors.

Test setup started with installation of the test stand, motor, rotor balance, and rotor hub in the whirl cage. For the SMART rotor test a hub mounted data acquisition and multiplexing system, Figure 14, and a slip ring for rotor data

and actuator power transfer were developed. For transmission. A total of 45 rotating system parameters, pitch link loads, flap loads, flap actuator system parameters included 5 balance loads, mast accelerometers, and flap actuator electrical data. A total of 130 parameters were recorded programming of the data acquisition and display systems.

to test the slip ring was mounted below the torsion. 23 blade bending and torsion displacements and loads, and piezo stack temperatures. Sixty fixed test stand displacement, control system loads and displacements, test stand tracked 25 systems and represented as a significant effort.

All flap inputs were made as direct voltage commands for processing of feedback signals, limit monitoring control modes was programmed in Simulink. Amplifier distribute and filter input commands, filter the high voltage actuator command outputs, and provide control, sensor, and shutdown circuits for the 28V power supplies.

using a Space controller card in a ruggedized PC. Software, automated shutdown, and the various open and closed loop control, sensor, and provide control, sensor, and shutdown circuits for the 28V power supplies.

The rotor was tested for 13 hours, including 7 hours of flap operation, under a range of conditions. Figures 15 and 16 show the rotor installed on the test stand. Initial runs were made for rotor tracking and balancing to 9 degrees, cyclic control sweeps up to ± 2 degrees, and rotor operated open loop with static and dynamic commands up to 107% overspeed. The flaps were ± 500 V and 6/rev (6P). The flap phasing was also varied. The flap showed excellent authority with oscillatory thrust. Various flap actuation frequency sweeps were run to investigate the dynamics of the rotor (up to 80 Hz) and the flap system (up to 400 Hz). Static operation of all flaps or one flap only were run to investigate the possibility of fusing the flaps for blade tracking. Test with static command to one flap and dynamic command to the other four flaps were run to simulate the case where one flap actuator was inoperative or experienced a hard-over. A few cases were run to explore closed loop commands, using either hub accelerations or balance loads for feedback. Last but not least, the active flap system was run continuously for over two hours without any performance or thermal issues.

rotor speed and collective when no voltage is applied to the flap deflection is zero; small differences due to flap rigging are not increasing. Taken individually, flaps 0.75 deg trailing edge down. Changing collective from 0 to 8 deg displace the flaps about 0.75 deg up.

Figure 17 shows the change in flap deflection with actuators. At zero speed and collective the flap deflection is zero; small differences due to flap rigging are not increasing. Taken individually, flaps 0.75 deg trailing edge down. Changing collective from 0 to 8 deg displace the flaps about 0.75 deg up.

Static flap inputs were made at 0, 4, and 8 degrees static voltage at 0 and 8 degrees. Applying 400V to certain amount of hysteresis in the flap deflection pitch link and blade torsion loads. It was also observed that the flap deflection is zero at 100% Rpm and 8 deg collective. Taken individually, flaps 0.75 deg trailing edge down. Changing collective from 0 to 8 deg displace the flaps about 0.75 deg up.

Static flap inputs were made at 0, 4, and 8 degrees static voltage at 0 and 8 degrees. Applying 400V to certain amount of hysteresis in the flap deflection pitch link and blade torsion loads. It was also observed that the flap deflection is zero at 100% Rpm and 8 deg collective. Taken individually, flaps 0.75 deg trailing edge down. Changing collective from 0 to 8 deg displace the flaps about 0.75 deg up.

Dynamic flap inputs were made at rotor speed multiple frequencies of 1/rev through 6/rev at a range of collective modes with all flaps receiving the same command data. The majority of runs were made in the 'harmonic' mode with flap inputs phased azimuthally such that each flap receives the same command at a given azimuth. Figures 20-22 show the cyclic flap deflection and harmonic component of blade torsion moment at static on 71 in and balance normal force at the excitation frequency for 8 deg collective and three voltage levels. Flap deflection amplitudes at ± 450 V are about 3 deg and approach 3.5 deg at 5P as a result of flap/torsion coupling, Figure 20. The flap inputs result in significant blade torsion cyclic loads at 1P and 2P, the effect of the fundamental torsion mode is evident.

The best indicator of flap authority in hover are changes in rotor thrust. Oscillatory thrust provides a direct assessment of changes in the blade aerodynamic loading due to blade geometry changes from flap inputs. Balance

Balance

normal force results, Figure 22, show that with harmonic loads are seen. Applying ± 450 V at 5 Presults in a thrust. This level of authority at a medium value systems should be able to provide the expected vibra-

tion, noise, and aerodynamic improvements in forward

ly 5/rev balance a steady state that the flap deflection.

One advantage of the flap system is that it is completely independent of the primary control system and that the system behavior with one flap in operation is normally. No problems were observed, but airframe to occur on an aircraft. To further demonstrate robustness, the system was run continuously for over two hours after completion of the whirl test the flap system was be data taken before the whirl test and no signs of an

interference or undue wear were found.

dis not flight at full static level vibration intensity, the same. After the match

6. SUMMARY

A full scale rotor system with piezoelectric actuator development effort included design, fabrication, and piezoelectric actuators, switching power amplifiers diameter rotor demonstrated the functionality, robustness, and required authority of the flap system.

blade flap was developed and whirl to be tested. The component testing of rotor blades, trailing edge, and the data/power system. Whirl to be tested to

. The flaps, the 34-foot

Proving the integration, robust operation, and authority of the flap system were the key objectives. The piezoelectric materials and actuator to the application and test results demonstrate the feasibility and practicality of applying smart materials for limited authority, active control on a helicopter rotor. Follow-on forward flight demonstrations in vibrations, noise, and aerodynamic performance. Extension of this technology are a prime candidate for on-blade flight control, i.e. elimination of the washplate.

Proving the integration, robust operation, and authority of the flap system were the key objectives. The piezoelectric materials and actuator to the application and test results demonstrate the feasibility and practicality of applying smart materials for limited authority, active control on a helicopter rotor. Follow-on forward flight demonstrations in vibrations, noise, and aerodynamic performance. Extension of this technology are a prime candidate for on-blade flight control, i.e. elimination of the washplate.

by the whirl and application of applying demonstrations performance. the washplate.

Specific conclusions are:

1. Model scale rotor tests demonstrated the feasibility and benefits of piezoelectric actuated trailing edge flaps.
2. High voltage custom piezo stacks can be driven at high field levels and mechanical preload without put s 75% larger than commercially available without affecting durability.
3. A high energy, compact piezoelectric actuator for operation in the rugged rotor blade environment was developed. Performance and durability were demonstrated in extensive bench tests.
4. A high efficiency switching power amplifier was developed. Power density was increased four-fold compared to previous models.
5. Aeroelastic simulation models for the flap system were developed. Results showed that 2 degrees of flap deflection are sufficient for vibration reduction at high speed.
6. The actuator/flap integration into the blade was optimized for performance, weight, matching baseline blade dynamics, and using production blade tooling. Fabrication methods were developed to embed actuator and flap in the blade.
7. The robustness and control authority of the flap system was demonstrated in whirl to be tests. The rotor was fully instrumented and an extensive data set of actuator performance and rotor loads was obtained.
8. Actuator authority exceeded requirements. Flap induced oscillatory rotor thrust was greater than 10% of baseline thrust.
9. The SMART rotor system is ready for forward flight demonstrations.

1. Model scale rotor tests demonstrated the feasibility and benefits of piezoelectric actuated trailing edge flaps.
2. High voltage custom piezo stacks can be driven at high field levels and mechanical preload without put s 75% larger than commercially available without affecting durability.
3. A high energy, compact piezoelectric actuator for operation in the rugged rotor blade environment was developed. Performance and durability were demonstrated in extensive bench tests.
4. A high efficiency switching power amplifier was developed. Power density was increased four-fold compared to previous models.
5. Aeroelastic simulation models for the flap system were developed. Results showed that 2 degrees of flap deflection are sufficient for vibration reduction at high speed.
6. The actuator/flap integration into the blade was optimized for performance, weight, matching baseline blade dynamics, and using production blade tooling. Fabrication methods were developed to embed actuator and flap in the blade.
7. The robustness and control authority of the flap system was demonstrated in whirl to be tests. The rotor was fully instrumented and an extensive data set of actuator performance and rotor loads was obtained.
8. Actuator authority exceeded requirements. Flap induced oscillatory rotor thrust was greater than 10% of baseline thrust.
9. The SMART rotor system is ready for forward flight demonstrations.

ACKNOWLEDGEMENTS

Drs. Ephraim Garcia and Terry Weisshaar, DARPA, provided the motivation and funding for the effort. Dr. Gary Anderson, ARO, provided technical oversight with support from other researchers at U.S. Army laboratories. Dr. Janet Sater, IDA, provided guidance. Drs. William Warmbrodt (NASA) and Chee Tung (U.S. Army) provided funding and technical oversight. At Boeing the following engineers, staff, and subcontractors provided support:

Dr. Gary Anderson, ARO, provided technical oversight with support from other researchers at U.S. Army laboratories. Dr. Janet Sater, IDA, provided guidance. Drs. William Warmbrodt (NASA) and Chee Tung (U.S. Army) provided funding and technical oversight. At Boeing the following engineers, staff, and subcontractors provided support:

Lou Silverthorn, Mike Nothaft, Jeff Hughes, Mike Gamble, Dave Domzalski, Joseph Jette, and many others. At the University of Maryland, Prof. Inderjit Chopra, assisted by Jinwei Shen, Taeh Lee, Andreas Bernhard, and Nikhil Koratkar supported rotor aeroelastic analyses and flap actuator spin testing, and conducted model rotor wind tunnel tests. At UCLA, Prof. Gregory Carman, assisted by Milan Mitrovich and Paul Chaplya, tested PEmaterials. At MIT, Prof. Steven Hall, assisted by Eric Prechtlan and Dora Tzianetopoulou, conducted model rotor spin tests and supported design of the double-x-frame actuator.

REFERENCES

1. Chopra I., "Status of Application of Smart Structures Technology to Rotorcraft Systems", RAEC Conference "Innovation in Rotorcraft Technology", London, UK, June 1997 (republished in Journal of the AHSSociety, Vol. 45(4), pp 228-252, October 2000).
2. Friedmann P., "The Promise of Adaptive Materials for Alleviating Aeroelastic Problems and Some Concerns," RAEC Conference "Innovation in Rotorcraft Technology", London, UK, June 1997.
3. Straub, F.K. and King, R.J., "Application of smart material to control of a helicopter rotor," Proc. SPIE Symposium on Smart Structures and Materials, San Diego, March 1996.
4. Hasegawa Y., Katayama N., Kobiki N., Nakasato E., Yamakawa E., Okawa H., "Experimental and Analytical Results of Whirl Tower Test of ATIC Full Scale Rotor System," 57th Annual Forum, Washington, DC, May 11, 2001.
5. Enekl, B., Klöppel, V., Preißler, D., and Jänker, P., "Full Scale Rotor with Piezoelectric Actuated Blade Flaps," Proc. 28th European Rotorcraft Forum, Paper 89, Bristol, UK, Sept. 2002.
6. Straub, F.K. et al., "Smart Material Actuated Rotor Technology - SMART," Proc. AIAASDM Conference, AIAA-2000-1715, Atlanta, GA, April 2000.
7. Precht, E., and Hall, S.R., "Closed-Loop Vibration Control Experiments on a Rotor with Blade Mounted Actuation," Proc. 41st AIAASDM Conference, AIAA-2000-1714, Atlanta, GA, April 2000.
8. Koratkar, N.A., and Chopra, I., "Wind Tunnel Testing of a Mach-Scaled Rotor Model with Trailing Edge Flaps," Proc. 57th AHS Annual Forum, Alexandria, VA, 2001, pp. 1069-1099.
9. Shen, J. and Chopra, I., "Aeroelastic Modeling of Trailing-Edge Flaps with Smart Material Actuators," Proc. 41st AIAASDM Conference, AIAA-2000-1622, Atlanta, GA, April 2000.
10. Shen, J. and Chopra, I., "Aeroelastic Stability of Smart Trailing-Edge Flap Helicopter Rotors," Proc. 42nd AIAASDM Conference, AIAA-2001-1675, Seattle, WA, April 2001.
11. Mitrovic, M., G.P. Carman, and F.K. Straub, "Electro-Mechanical Characterization of Piezoelectric Stack Actuators," Proc. SPIE Conference on Smart Structures and Materials, SPIE Vol. 3668, Newport Beach, CA, March 1999, pp. 586-601.
12. Mitrovic, M., Greg P. Carman, G.P. and Straub, F.K., "Durability Characterization of Piezoelectric Stack Actuators under Combined Electro-Mechanical Loading," Proc. AIAASDM Conference, AIAA-2000-1500, Atlanta, April 2000.
13. Mitrovic, M., G.P. Carman, and F.K. Straub, "Durability of Piezoelectric Stack Actuators under Combined Electro-Mechanical-Thermal Loading," Proc. SPIE Conference on Smart Structures and Materials, Paper 4333-04, Newport Beach, CA, March 2001, pp. 586-601.
14. Chaplya, P.M. and Carman, G.P., "The Effect of Mechanical Prestress on Dielectric and Piezoelectric Response of PZT-5H at High Electric Fields," Adaptive Structures and Material Systems, Orlando, FL, Nov. 2000, pp. 327-334.
15. Chaplya, P. and Carman, G.P., "Dielectric and Piezoelectric Response of Lead Zirconate Titanate at High Electric and Mechanical Loads in Terms of Non-180 Degree Domain Wall Motion," Journal of Applied Physics, November 2001, V90 Issue 10, pp. 5278-5286.
16. Hall, S.R., Tzianetopoulou, T., Straub, F.K., and Nago, H., "Design and Testing of a Double X-Frame Piezoelectric Actuator," Proc. SPIE Conference on Smart Structures and Materials, Newport Beach, CA, March 2000.
17. Clingman, D.J., and Gamble, M. "High Power Piezoelectric Amplifier for Large Stack and PFC Applications," Proc. SPIE Conference on Smart Structures and Materials, Newport Beach, CA, March 2001.

Table1:Rotorcharacteristics

Rotorblade	modifiedMD900
Hubtype	bearingless
No.ofblades	5
Radius	203.1in
RotorSpeed	392rpm
Chord	10in
Airfoil	HH-10,HH-06
Twist	10deg
Torsionfrequency	5.7/rev

Table2:Flapdata

Radialstation	150–186in
Length	36in
Chord	3.5in
Hingelocation	75%ofchord
Hornlength	0.75in
Max.flapangle	±6deg

Table3:2x-Frameactuatorcharacteristics

Blockedforce	113lb
Freestroke	0.081in
Maximumwork	2.28in-lb
Voltage	475±725V
Weight	2.16lb
Specificwork	1.1in-lb/lb

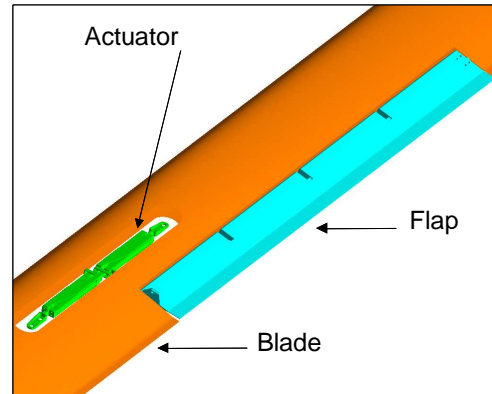


Figure 1:MD900bladewithembeddedpiezoelectric actuatorandtrailingedgeflap

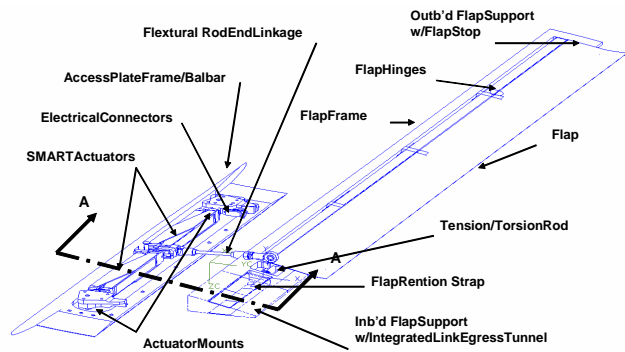


Figure 2:Blade,flap,actuatordesignintegration

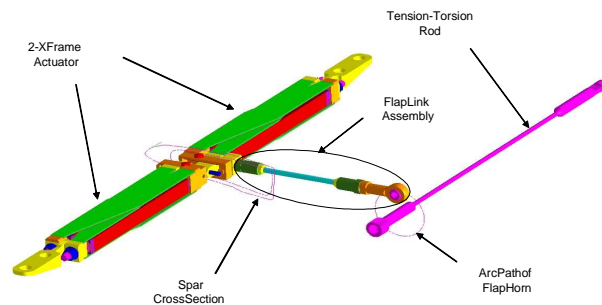


Figure 3:Actuator,flaplink,tension-torsionrod

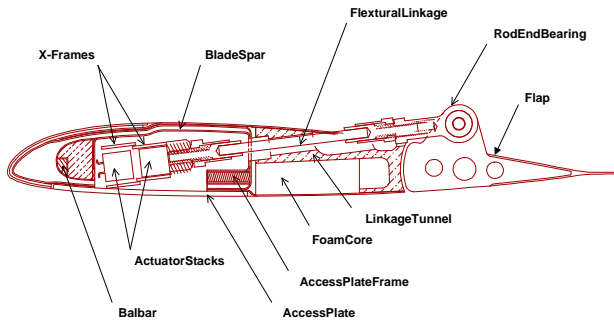


Figure 4: Blade, flap, actuator cross-section (A-A)

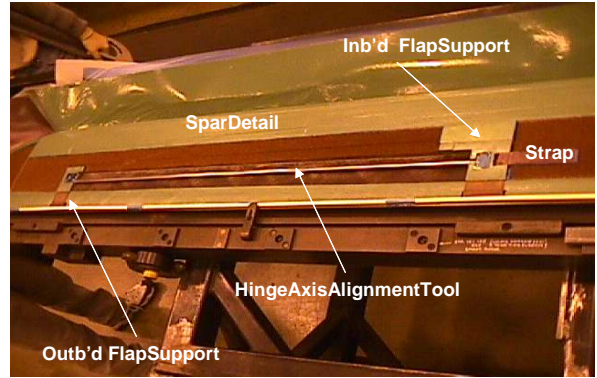


Figure 7: Bladespar and flap support detail layout

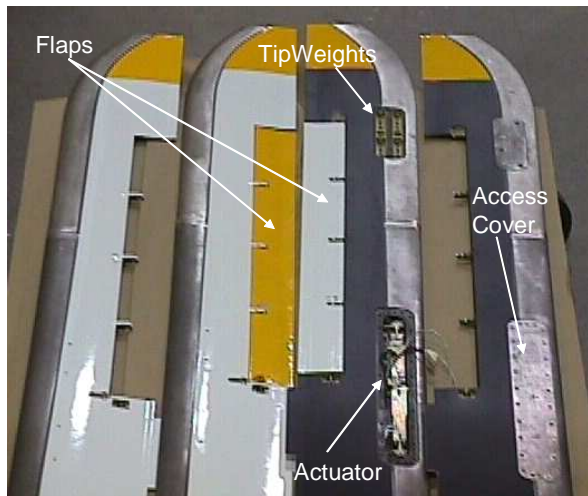


Figure 5: Flap system components

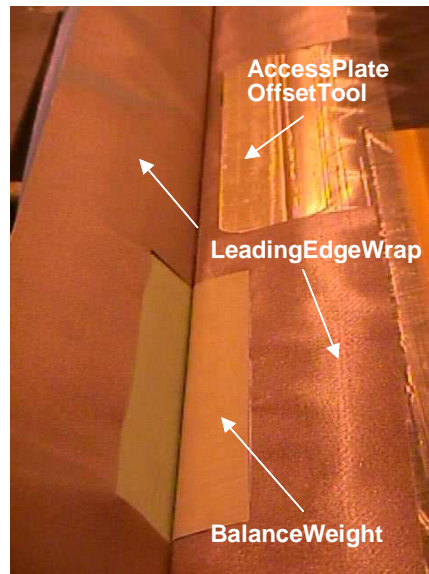


Figure 8: Leading edge wrap closure and balance weight

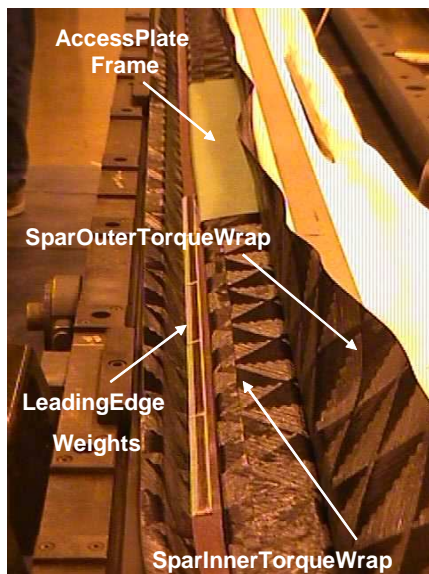


Figure 6: Bladespar fabrication

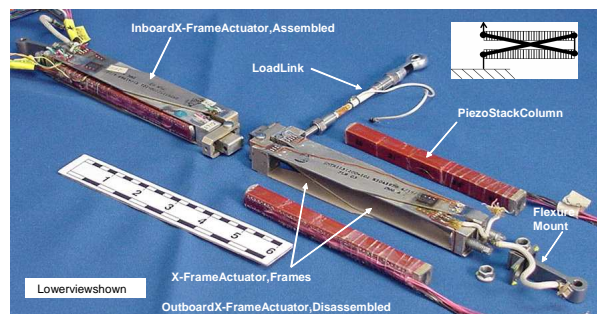


Figure 9: 2x-frame actuator

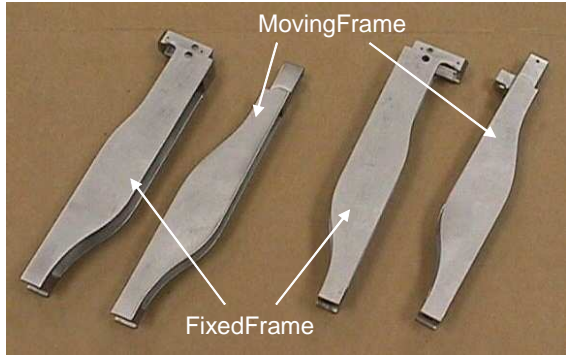


Figure 10: 2x-frame actuator details

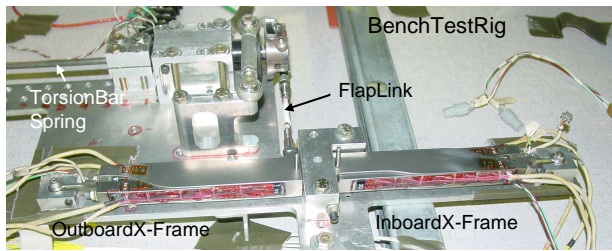


Figure 11: Actuator on bench test rig

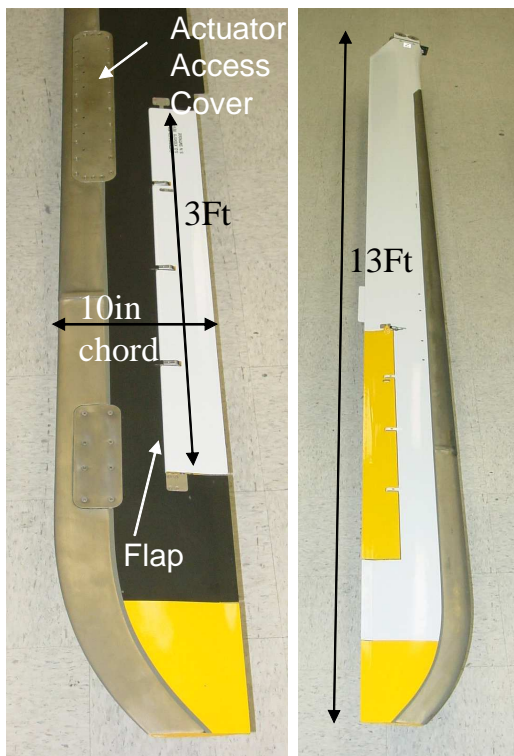


Figure 12: Smart rotor blade assembly

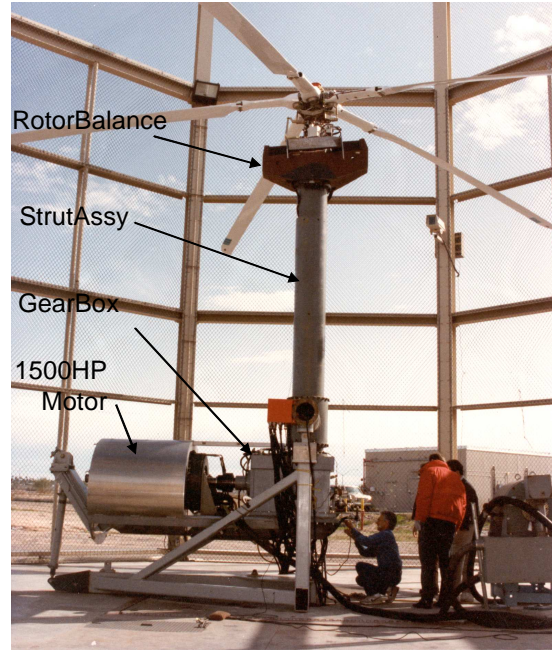


Figure 13: Larger rotor test stand (LRTS)



Figure 14: Rotor hub with data/power transfer unit



Figure 15: Smart rotor blade on whirl tower

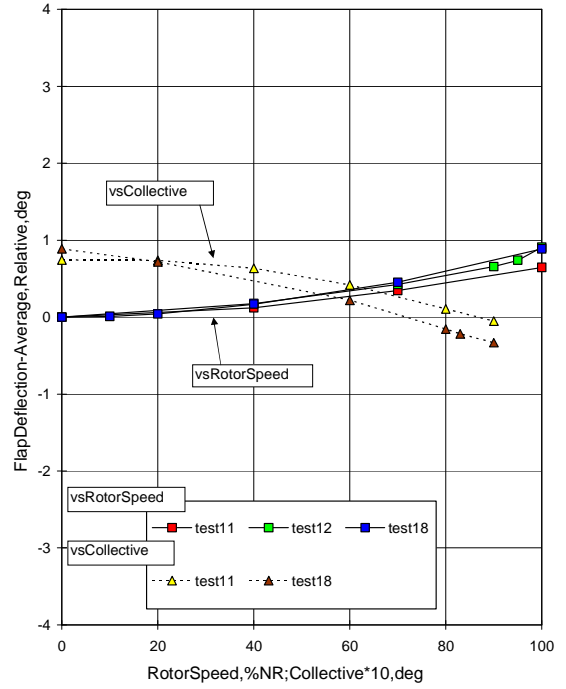


Figure 17: Flap deflection versus rotor speed (0 deg collective) and collective pitch (100% Rpm) with no power applied.



Figure 16: Smart rotor on whirl tower

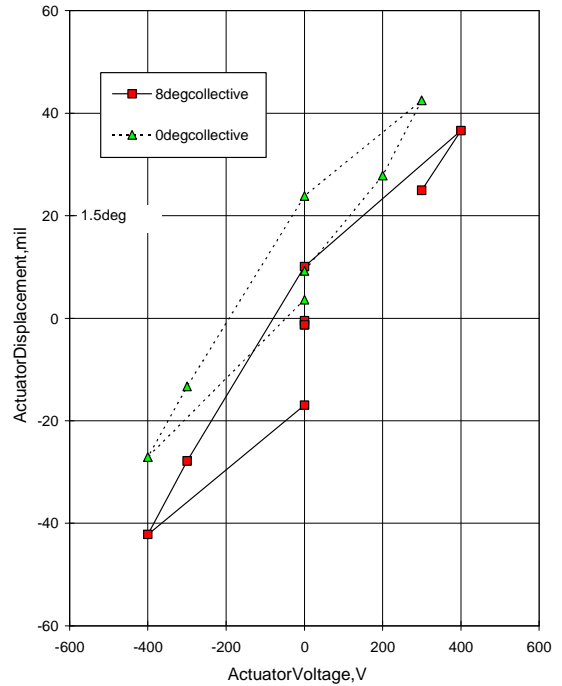


Figure 18: Static actuator deflection versus applied voltage, at 100% Rpm

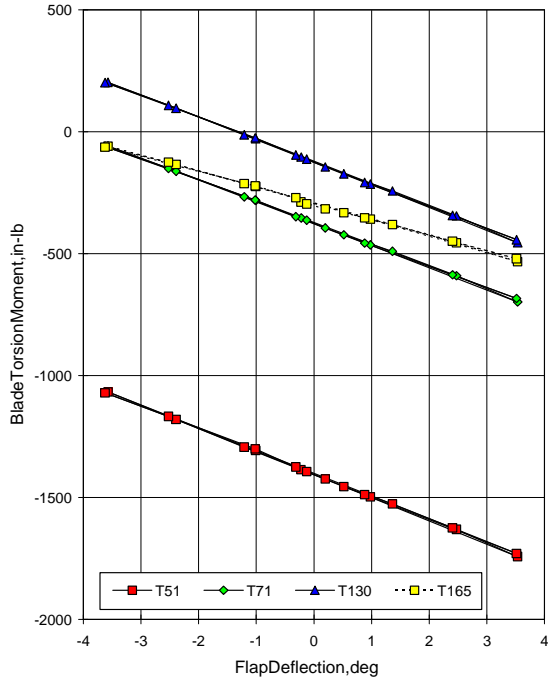


Figure 19: Blade torsion moment at four stations versus static flap deflection (8 deg coll., 100% Rpm)

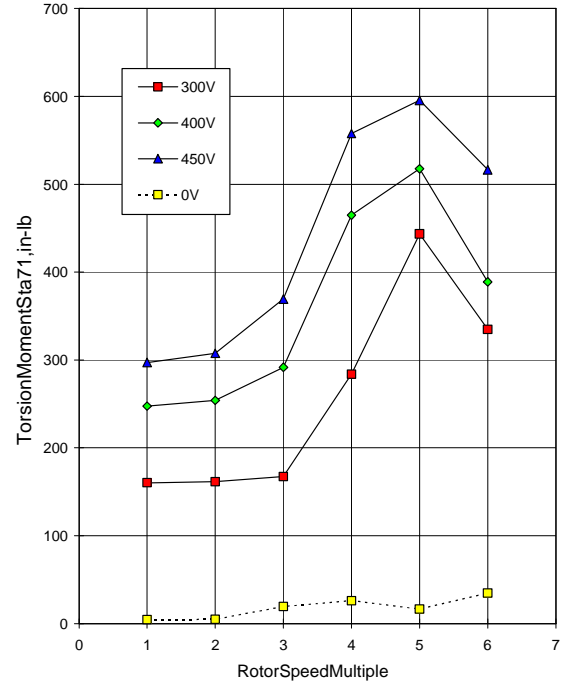


Figure 21: Blade torsion moment harmonics at station 71 in the excitation frequency for three voltage levels (100% Rpm, 8 deg collective, 1P=6.53Hz)

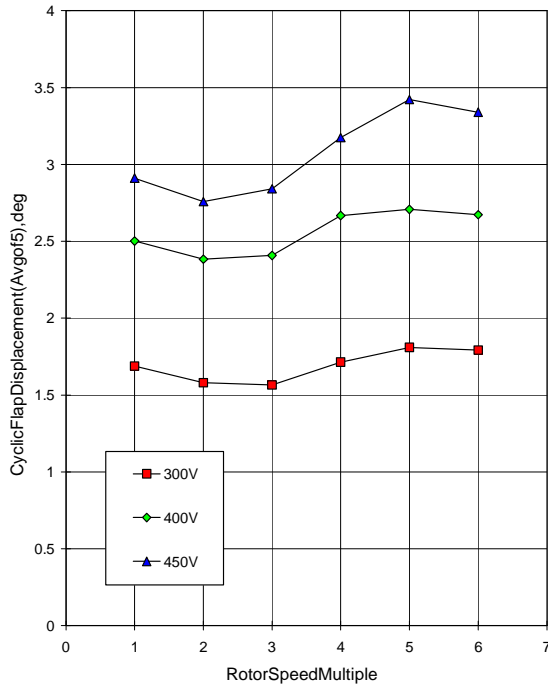


Figure 20: Flap deflection versus excitation frequency for three voltage levels (100% Rpm, 8 deg collective, 1P=6.53Hz)

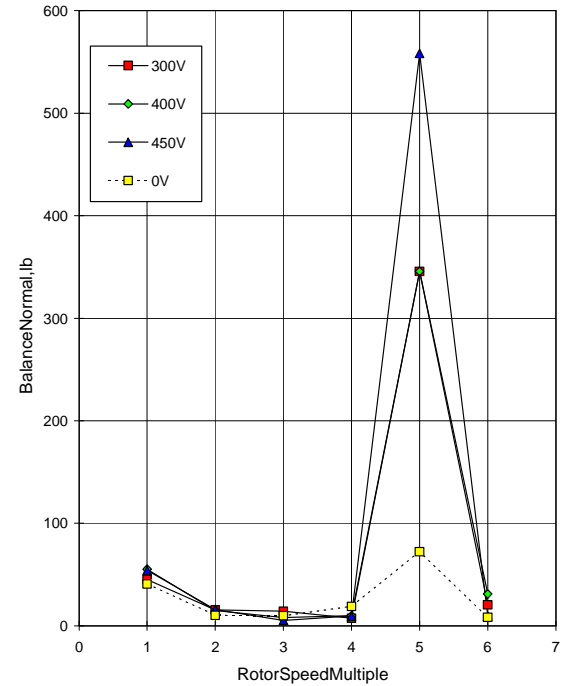


Figure 22: Balance normal force (thrust) harmonics at the excitation frequency for three voltage levels (100% Rpm, 8 deg collective, 1P=6.53Hz)